THE BALTIC JOURNAL
OF ROAD
AND BRIDGE
ENGINEERING
2022/17(4)

ISSN 1822-427X/eISSN 1822-4288
2022 Volume 17 Issue 4: 146–170
https://doi.org/10.7250/bjrbe.2022-17.583

DYNAMIC STRAY CURRENT MEASURING METHODS IN URBAN AREAS

KATARINA VRANEŠIĆ[1*], MARIJANA SERDAR[1], STJEPAN LAKUŠIĆ[1], VÁCLAV KOLÁŘ[2], ANDREA MARISCOTTI[3]

[1]*University of Zagreb, Faculty of Civil Engineering, Zagreb, Croatia*

[2]*VŠB-Technical University of Ostrava Department of Electrical Engineering, Ostrava, Czech Republic*

[3]*University of Genoa, Department of Electrical, Electronic and Telecommunications Engineering, and Naval Architecture, Genoa, Italy*

Received 4 January 2022; accepted 11 July 2022

Abstract. In areas where urban tracks are used as public transportation, dynamic stray currents cause high maintenance costs for the tracks and metal structures near the tracks. Stray currents caused by rail vehicles depend on many factors (traffic density, vehicle speed, acceleration and deceleration, soil and track moisture), so it is very difficult to get a clear picture of the harmfulness of the stray current based on the results of a single field measurement. However, there are several measurement methods that can be used to determine the presence of stray currents and predict appropriate track maintenance actions. Some of these methods are described in this article, namely the use of stray current mapper, measurement of rail potential and rail

* Corresponding author. E-mail: kvranesic@grad.hr

Katarina VRANEŠIĆ (ORCID ID 0000-0001-7610-3469)
Marijana SERDAR (ORCID ID 0000-0001-8386-7272)
Stjepan LAKUŠIĆ (ORCID ID 0000-0002-5407-9290)
Václav KOLÁŘ (ORCID ID 0000-0002-4626-9844)
Andrea MARISCOTTI (ORCID ID 0000-0002-0096-7305)

current, measurement at the stray current collection system, and the use of non-destructive sensors. In track construction, measuring the electrical potential between rail and ground is one of the most common methods of detecting the damaging influence of stray current.

Keywords: rail current, rail potential, stray current mapper, stray current, stray current measurement, stray current corrosion, urban tracks.

Introduction

Stray current represents current that is flowing into the ground from insufficient isolated conductor resulting with the stray current corrosion (Siranec et al., 2019). Stray current leaks through the path of the smallest resistance and it can originate from different sources. Stray current can be static and dynamic. Sources of static stray current are offshore structures, marine platforms, cathodic protection systems, and the main source of dynamic current is electrical traction system (Siranec et al., 2019). Unlike industrial platforms that produce stray current with a relatively stable intensity in time, stray currents produced by electrical tractions are fluctuating in intensity and duration. They may fluctuate over short or long intervals of time, parallel to the varying load of the power source. The biggest intensity of stray current will be during the highest traffic load (morning and afternoon rush hours) (Chen et al., 2017). Stray current arising from electrified traction systems may be direct (DC) stray current or alternating (AC) stray current. Influence of AC current is much less dangerous than DC current (Chen et al., 2017).

Tramways and subways are operated at DC with nominal voltage in the range of 500 to 1500 V, most commonly in the lower rage of it, namely 600 to 750 V (Steimel, 2012; Krajcar et al., 2009). The vehicles receive power through the pantograph and the so-formed current path recloses back to the Traction Power Stations (TPSs) through the running rails (Krajcar et al., 2009; Dolara & Leva, 2009). Rails are not grounded and feature some amount of electrical insulation to prevent leakage of traction current. At the same time, their instantaneous potential may reach higher values than for a fully grounded solution, so that there is always some compromise between stray current protection and electrical safety (touch voltage) (Mariscotti, 2021a).

When the traction current flows back to the TPS, a potential is created between the rails and the earth due to the longitudinal resistance (or, in general, impedance) of the rails themselves; such rail potential is variable along the track and, in general, minimum at TPSs (Du et al., 2016). Since it is very difficult to isolate the rails completely, some of the return current leaks away from the rails and reaches the

TPS from alternative paths. This current is called stray current. Such paths attract stray current because they may be conveniently less resistive, e.g., because of their large cross-section (the soil itself) (Du et al., 2016; Hill & Cai, 1993). If a pipeline crosses a railway system, stray current may be picked up at the points of crossing as trains pass. Current will flow in both directions from the crossings and discharge at remote locations. On the other hand, if the pipeline is parallel with the rails, but does not approach a DC substation, it will pick up current as the tram track vehicle passes the parallel section. This current may be discharged from the ends of the parallel section. In finding its way back to the DC substation, stray current may flow from pipeline to pipeline, at crossings, in order to follow the least resistant path (Hartenergy, 2021; Alamuti, et al. 2011). This phenomenon is particularly relevant in an urban context, such as for tram lines because the soil is full of structures and low-resistance paths (pipes, reservoirs, cables, walls, foundations, etc.), tram tracks are almost all built in closed formation, and rails are not completely insulated.

At the point where the current leaves the rail or a metal object near the track, the anodic corrosion reaction (oxidation, dissolution of the metal) starts and at the point where the current enters the rail or another metal object, the cathodic part of the corrosion reaction takes place (Zaboli et al., 2017).

Stray current magnitude depends on the traction current, the rail resistance and rail-to-earth resistance (Charalambous et al., 2016). Shape and material properties of rails are chosen with mechanical requirements as the main objective, and electrical characteristics are more or less in the background, as pointed out among others by Dolara & Leva (2009) and Mariscotti (2021b). The rail resistance affects the voltage drop and stray current leakage (Mariscotti, 2021b). According to Milesevic et al. (2018), the return current in the rails near electric traction substations and vehicles is about 75% of the supply current and decreases with distance from the contact points. The amplitude of the return current changes significantly only near the traction substations and vehicles. In the middle of the supply segment, return current has almost constant values. It depends on the rail-to-earth resistance. It reaches 53% of the feeder current at a ground resistance of 100 Ω and 59% of the feeder current at a ground resistance of 1000 Ωm (Milesevic et al., 2018).

The highest stray current values occur on tracks with discretely fastened rails (Figure 1a) when the fasteners are not insulated from the

rail. When these tracks are constructed as part of the roadway surface and closed with various materials (asphalt, concrete slabs, etc.), it is very difficult to provide adequate drainage, so water keeping will increase stray current values. In continuously supported and fastened tracks (Figure 1b), the rails are completely insulated, and a high electrical resistance is obtained between the rail and the ground, so that the current cannot leak from the rail. In this type of track, the rails are laid in the grooves of the precast concrete slab and the free space between the rail and the slab is filled with elastic material so that the rails are separated from the surrounding structure and protected from corrosion processes (Vranešić et al., 2020).

Measures to reduce stray current at the source can be divided into two groups: Reducing the longitudinal rail resistance and increasing the resistance between rail and earth (Wang et al., 2020). The electrical resistance of the rail depends on many factors – type of rail, distance between electrical substations, rail cross-section. The value of longitudinal rail resistance is 40–80 mΩ/km (Charalambous, 2005). The values of the stray currents depend on the electrical resistance between rail and earth. This resistance depends on the type of fastenings and sleepers, the use of insulating materials and their performance, the type of track construction and the type of soil (Bongiorno & Mariscotti, 2015).

To prevent the current from entering the buried metal object near the track, stray current collection systems are installed on many urban tracks in order to collect the current flowing off the rails and return it to the electrical substation (Xu & Wang, 2013).

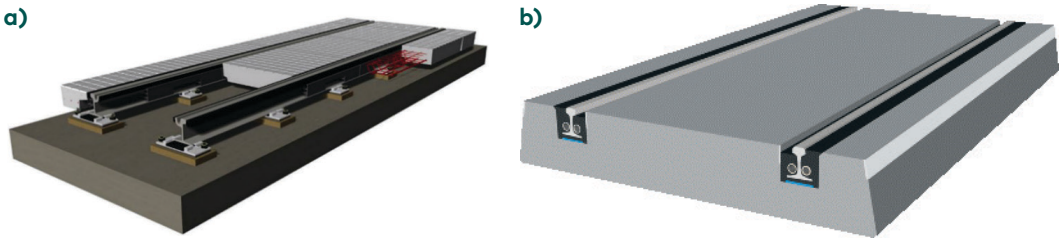

Figure 1. a) Model of discretely supported and discretely fastened track, b) Model of continuous supported and fastened track (Vranešić et al., 2020)

1. Rail corrosion: Examples and case studies

1.1. Examples of rail corrosion

Rail corrosion is a consequence of stray current and rail contact with the corrosive environment. Robles Hernández et al. (2009), Safa et al. (2015), Isozaki et al. (2016) and Xu et al. (2021) analysed electrochemical corrosion at the rail foot in urban tracks. Rail corrosion failure usually occurs at the rail foot. Tracks with discretely supported rails are most susceptible to corrosion processes, as the corrosive media can easily accumulate in the region of the rail foot. The fastening system acts as a barrier to the flow of the corrosive media, so that the greatest corrosion damage occurs at the contact between rail and fastening (Panda et al., 2008). Corrosion at the rail foot leads to thinning of the rail cross-section and instability of the rail with the risk of displacement and accumulating the large stresses or even failure of the rail (Xu et al., 2021). Loss of material at the rail fastening and at the top and bottom of the rail foot can also reduce fastener toe load and affect traffic safety. This can increase the possibility of rail rollover or track widening on sharp curves (TCRP, 2016). In closed rail formation, the rail foot thickness can only be determined when the track is open, which in some cases is not done until the track is reconstructed. Figure 2 shows examples of rail corrosion noticed during track reconstruction.

In closed track systems, it is very difficult to insulate the rail completely, so the corrosion process can be very rapid. Furthermore, if proper track drainage is not provided, water remaining in the track will accelerate corrosion. Urban tracks built into road surface are also exposed to chlorides, which are used in winter to prevent icing of the

Figure 2. Rail degradation noticed at urban tracks

road surface (Safa et al., 2015). These chlorides dissolve easily in water and enter the track. Figure 3 shows the condition within the closed track formation, and this condition is present through the most part of the year. This is noticed during reconstruction, after the track was opened.

At the places where current is leaving from the rail, material loss at the rail and rail fastening is much higher due to stray current corrosion. This type of corrosion is different from natural corrosion because it is caused by an external electrical current (WebCorr, 2021; Alar, 2015). Stray currents may have more serious consequences in chloride-contaminated medium due to higher electrical conductance of this medium (Chen et al., 2017). Zaboli et al. (2017) made numerical analysis of stray currents at the fastening point considering different values of rail-to-earth resistance. Three different models were analysed and the only difference between the models was the value of soil resistivity – in model A the soil resistivity was 100 Ωm, in model B – 300 Ωm and in model C – 1000 Ωm. The type of rail fastening system was the same in all three models. The results showed that the stray currents were the highest in model A because the electrical resistance between the rail and the ground was very low due to low soil resistivity. For discretely fastened tracks, these models can be identified with electrical resistance between the rail and the ground at the points where the rail is fixed to the base. At these locations, the resistance between the rail and the ground is a function of the insulation of the fastening system (Charalambous, 2017).

When the fastening system is isolated from the rail, the resistance between the rail and the ground is high. If, on the other hand, the fastening system is in direct contact with the rail, current flows from the rail through the fastening system in the lower parts of the track.

Figure 3. Condition of the closed track formation during the most part of year

1.2. Measurement methods to detect rail corrosion

Many studies have been conducted on rail wear and defects, contact impact, and fatigue of rail materials, but most of them do not consider the effects of corrosion on rails (Xu et al., 2021; Ovchinnikov et al., 2021; Haladin et al., 2019). Conditions including sunlight, humidity, temperature, salt deposition affect corrosion (Xu et al., 2021), the change of temperature on rail surface, condensation of water from air and evaporation result in wet/dry cycle that also favours corrosion (Xu et al., 2021).

Samal et al. (2011) carried out corrosion tests on rails in different media – 3.4% NaCl at 45 and 65 °C and in sulfate medium (H_2SO_4, pH 1.49) at 45 and 65°C. It was found that the corrosion rate of the rail in a 3.4% NaCl solution at room temperature was 0.425 mm/year and as the temperature increased, the corrosion rate increased in the saline atmosphere. A sulfate medium with a pH of 1.59 can also cause corrosion. As the corrosion rate increases, the yield strength and tensile strength decrease. The presence of salt on the rails compromises the integrity of the rails because salt from the electrolyte promotes the reaction of oxygen with the rails, which leads to acceleration of corrosion. Most parts of the tracks are usually wet, so there is always contact between the rail, the fastening system and the electrolyte (Ritter et. al., 2018.

In a highly corrosive environment and in the presence of stray current, the service life of rails can be reduced to only a few years, so it is important to identify susceptible areas of track infrastructure and stop corrosion on time. For this reason, it is necessary to implement measurement methods to detect rail corrosion (Robles Hernández et al., 2009). Visual inspection is the primary method for corrosion detection at the rail foot, but it is only applicable to the open tracks (Ritter et. al., 2018). Developing non-destructive and contactless technologies of corrosion detection is necessary. Some operators are using ultrasonic detection and infrared inspection to detect rail corrosion. Xu et al. (2021) and Pathak et al. (2019) described a conceptual technique based on finite element simulations of the propagation of laser induced ultrasonic guided waves to detect cracks in the rail foot. High powered laser positioned above rail surface producing ultrasonic waves combined with an air-coupled transducer receiving ultrasonic signal can detect flaws within and under rails on an entire rail section (Xu et al., 2021).

Infrared inspection is also used to detect rail corrosion because of its ability to localize defects based on various thermal properties. Since localized corrosion in early stages cannot be detected by visual inspection, ultrasonic defect detection with ultrasound has been used

to detect non-visible surface fractures and internal defects and to assess corrosion at the rail foot (Xu et al., 2021). Some other non-destructive detection technologies used for rail corrosion detection are radiographic inspection, eddy current inspection, electromagnetic transducer, ground penetrating radar, etc. (Xu et al., 2021). These techniques have application prospect for rail corrosion, but there are still difficulties on implementation.

Robles Hernández et al. (2009) conduced numerical simulations of two corroded rail samples. The digitized image was imported into ANSYS software and used to create a highly reliable model that accurately reproduced the properties of the corroded rail. During the exploitation both rail samples were located on a sleeper and exposed to DC stray current. Corrosion was found to cause very complicated defect shapes that grew in unpredictable directions and caused sharp angles, resulting in significant stress concentration. The stress level can be high enough to easily lead to failure of the rail due to traffic load, as the cyclic stresses can reach values close to or above the yield strength of this steel.

2. Stray current measuring methods

The amount of stray current depends on the current in the rail, track construction techniques, and insulation techniques (Mariscotti, 2020). Stray currents are usually measured in buried pipelines to determine whether the pipelines are at risk from static or dynamic stray currents. Measurements of dynamic stray currents in railway infrastructure are not common in the literature and some measurement methods are difficult to perform due to the nature of the railway infrastructure (e.g., in a closed track system) and due to the high traffic load. Results of field measurements of stray currents or some other parameters used to calculate stray currents are subject to external influences. The relationship between the track potential distribution and the resulting stray current is an indicator of track isolation and stray current intensity. The value of rail-to-earth potential mainly depends on the number of vehicles on the track, load current, distance between traction substations, contact resistances between rail and earth, etc. (Zhang, 2012). The distribution of track potential is not intuitive, and several factors affect its waveform (Mariscotti, 2020):

- Traction and braking phases alternate, interrupted by coasting and deceleration phases;
- Rails and tracks are connected along the line (rail-to-rail and track-to-track), achieving optimal track balancing and allowing a

wide exchange of regenerative braking current towards traction units on the same or different tracks;
- Substations are approximately evenly distributed along the line and situations with one-way fed trains do not occur.

Ooagu et al. (2019) conduced measurement of rail potential in 7 electrical substations. Of these, 5 substations were located in urban areas and the other 2 were located in suburban areas. The measurement results showed that the rail potential of substations in urban areas was positive during most of the time of train operation and the rail potential of substations in suburban areas was negative during most of the time of train operation. This means that the current flows from the rails to the ground in the high-density train operation area and is sucked from the ground to the rails in the low-density train operation area. Ooagu et al. (2019) also conduced continuous measurement of rail potential in one substation for one year. It was established that the output current increased on hot and cold days and that the rail potential increased towards negative polarity especially on a cold day. By continuously measuring the rail potential in one substation it was confirmed that two factors affected the variation of rail potential. First, as the substation output current increases, the leakage current from the feeder circuit to ground increases and the rail potential becomes negative. Second, when the rail leakage resistance decreases due to rain, the leakage current increases and the rail potential becomes negative.

Many different methods are used today to detect dynamic stray current. Stray current can be detected at railway infrastructure or in

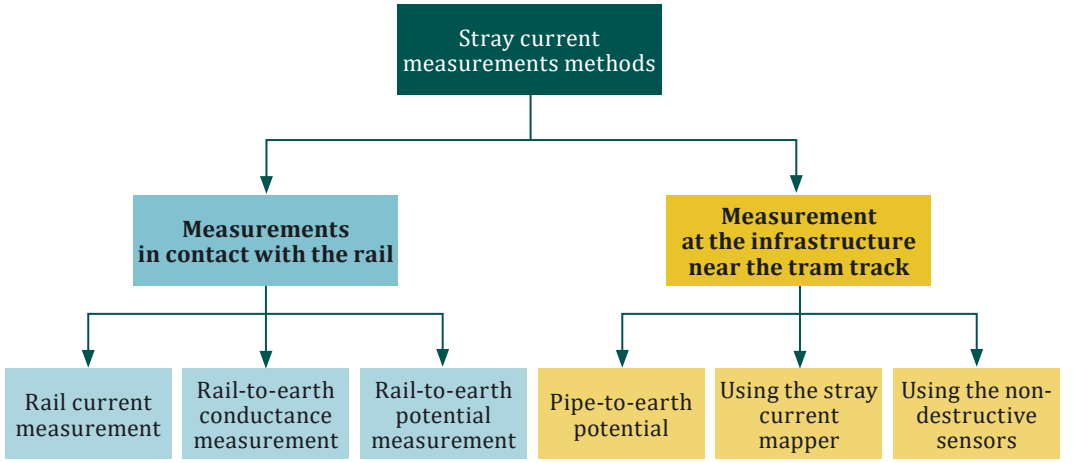

Figure 4. Stray current detection methods

buried metal objects that are endanger with the stray current. Accurate stray current measurement is the basis for stray current corrosion analysis, but stray current cannot be measured directly and indirect measurements are used to reflect stray current corrosion (Mariscotti et al., 2012; Peng et al., 2020).

Detection of stray current interactions is usually done by potential measurements. The structure potential value and its variability are adopted as criteria of the electrolytic corrosion hazards (Darowicki & Zakowski, 2004). Some of the most applicable measurement methods used to detect stray current are shown in Figure 4 and described in this paper.

Conductance per unit length between running rails and earth is the most critical parameter to consider in the design of an electrified railway system. Standard EN 50122-2:2011 defines the maximum allowable values of rail-to-earth conductance and potential:

- For open formation $G'_{\mathrm{RE}} \leq 0.5$ S/km per track and $U'_{\mathrm{RE}} \leq +5$ V;
- For closed formation $G'_{\mathrm{RE}} \leq 2.5$ S/km per track and $U'_{\mathrm{RE}} \leq +1$ V.

3. Preliminary measurements using stray current mapper

As the dynamic stray current from the rail penetrates through the soil into the buried infrastructure near the urban tracks, stray current can be measured in the buried infrastructure using the stray current mapper (SCM). SCM is a portable tool that uses sensitive magnetometers, which have a wide dynamic range and can separate currents in the milliamp range from other large current sources such as the earth's magnetic field. To measure the current, the sensor bar magnetometers locate pipe in the horizontal and vertical planes (Radiodetection, 2011), but before starting the measurement, it is necessary to obtain utility/substructure maps that show where all metallic underground pipelines are situated. This will greatly assist in mapping the area with the SCM.

SCM is equipped to measure static and dynamic stray current and has data logger to take continuous measurement over time. The SCM sampling frequency is 20 Hz. The current flow along the pipeline causes an electromagnetic field; therefore, the SCM can be used to detect the current in the buried metal infrastructure (Ivanković et al., 2009). Since the ground as well as dirt and sand, water, asphalt and concrete do not affect the electromagnetic field, the measurement is performed by placing the SCM device on the ground surface directly above the buried pipeline (Figure 5a) where the measurement is made (Ivanković et al., 2009). During the measurement, the data can be recorded on

the memory card in SCM device or directly to the computer. The measurement with the SCM is shown in Figure 5b.

During the measurement, the current in a buried infrastructure is continuously recorded and the software on the computer indicates with a bold arrow whether the current is flowing in the same direction as the red arrow on the SCM Sensor Bar or in the opposite direction (Radiodetection, 2011). Ivanković et al. (2011) found that it was possible to detect the influence of stray currents on buried pipelines using the SCM. The measurement performed by Ivanković et al. (2011) was carried out in the vicinity of the tramway infrastructure and during the data analysis a repetition of the current peaks was observed. To determine the current caused by the tram vehicle with the SCM, it is useful to record the passage time of the tram at the measuring point, so that during the data analysis it can be determined which current values are caused by which tram vehicle. The measurement with the SCM device was carried out in the city of Zagreb at two measurement points in Savska street, above the buried water pipelines. At these points, buried pipelines run parallel to the tram track infrastructure, which was determined by analysing the site plan of the water pipelines and tram

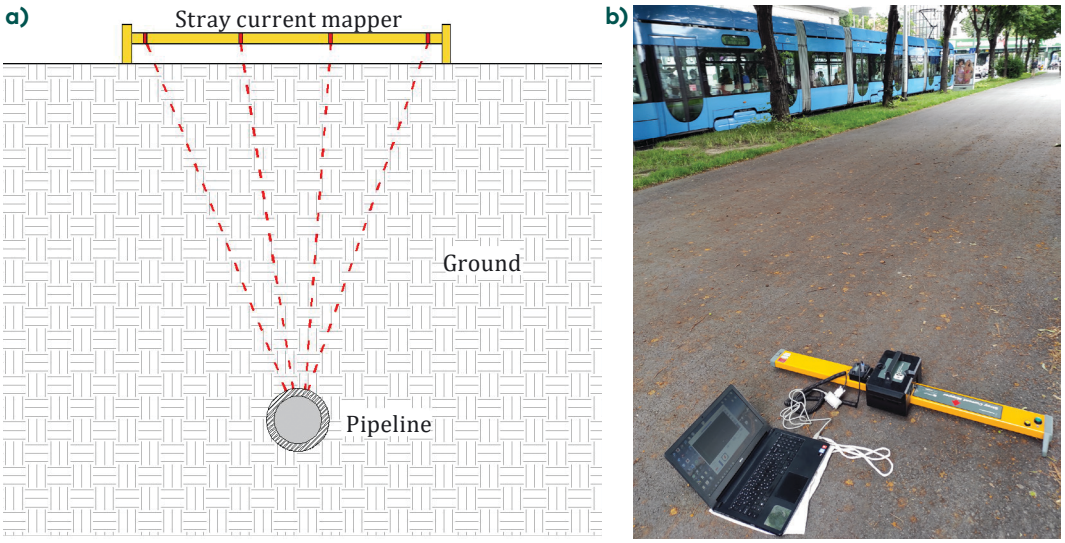

Figure 5. a) Schematic representation of the measurements with the SCM device, b) Stray current sensor bar during the measurement, SCM is connected directly to the laptop

track infrastructure. During the measurement, the times and types of all passing trams were recorded. Three types of trams were passing the measurement points, namely: TMK 2200, KT4, T4 (Figure 6).

The most important characteristic of a vehicle when it comes to stray current is the power that the vehicle requires to run. The power also determines how much current the vehicle draws from the power grid, and consequently the values of the return current in the rails. The characteristics of the above tram track vehicles are listed in Table 1.

Since the tram track at these two measurement points is built as part of the road surface, the passage time of each recorded tram vehicle is different and depends on the movement of the road vehicles as well as the light signals. Therefore, each vehicle accelerates and decelerates differently and drives at different speeds. The measurement period at each location was 10 min, because according to Mariscotti (2020) 10 min is a sufficiently long period to obtain significant information. During the measurement, 8 tram passes were recorded at measurement point 1 and 7 passes were recorded at measurement point 2. Due to the relatively low density of tram traffic during the measurement, it is easy to relate the values of the stray currents to the passage of a tram vehicle. The

Table 1. Characteristics of tram vehicles

Type of the tram vehicle	TMK 2200	KT4	T4
Power, kW	6 × 70	4 × 45	4 × 40
Voltage, V	600 (+20% – 30%)	600	600

Figure 6. Types of the tram vehicles that were passing the measuring points during the field measurement: a) TMK2200, b) KT4, c) T4 (Haladin et al., 2021)

results of this measurement are shown in Figure 7. As can be seen in the figure, each passing tram causes peaks in the graphs, and since the tram TMK 2200 consumes more current when driving than the KT4 and T4 tram, this results in a larger value of stray current.

At these two measuring locations, tram traffic is relatively sparse, so peaks in the curve caused by passing trams were easy to detect in the data analysis. When traffic is heavy, it is not possible to correlate the passing tram with the measured current. Figure 8 shows a diagram of stray currents in time also recorded at the buried pipeline in Savska street during the rush hour, when the traffic load was very high, and at night, when there was no tram traffic. During a 10-minute measurement

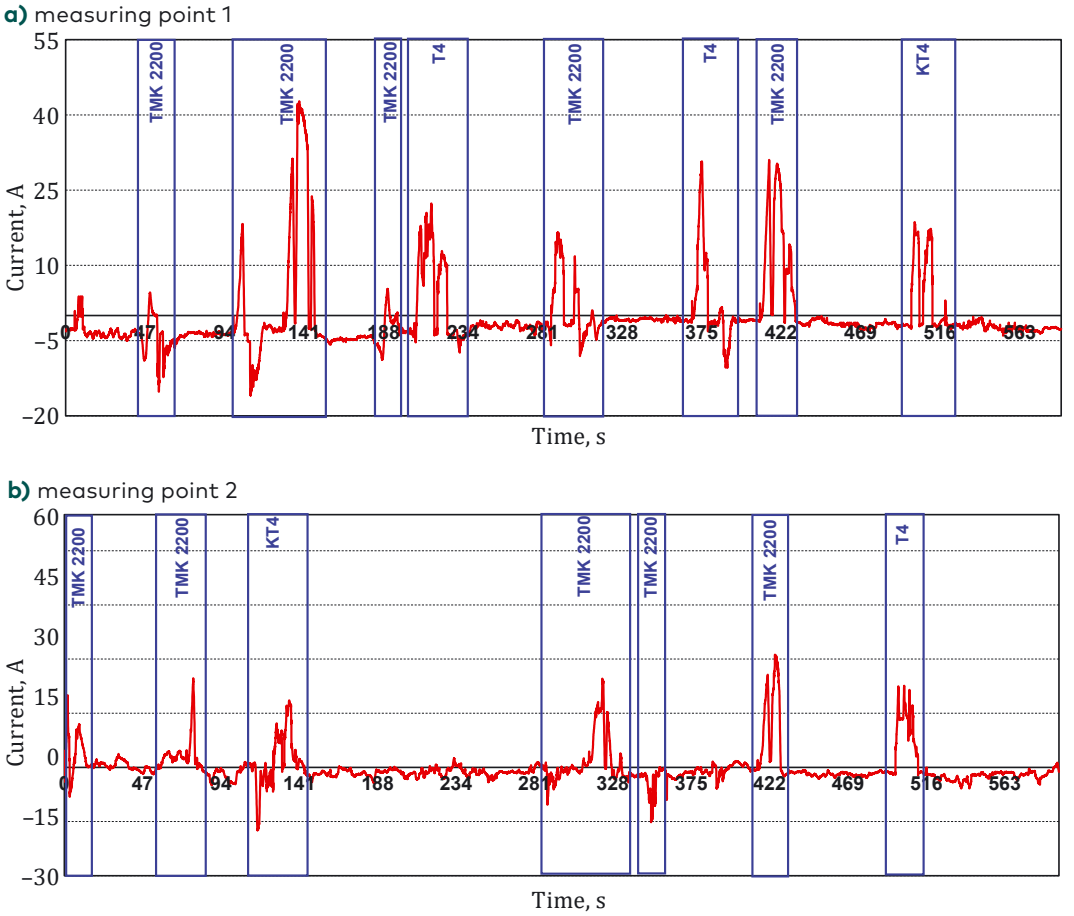

Figure 7. Results of stray current field measurement in two measuring points, with marked tram passes

period at rush hour, 24 tram passes were recorded. By overlapping the results from the daytime and night-time measurements, it was determined that all recorded currents were caused by tram traffic.

With the SCM device, it is possible to perform a preliminary measurement of the dynamic stray current on buried infrastructure in the vicinity of the tracks and, based on the results, to identify track sections that require further monitoring and to predict further track maintenance measures and methods to reduce stray current.

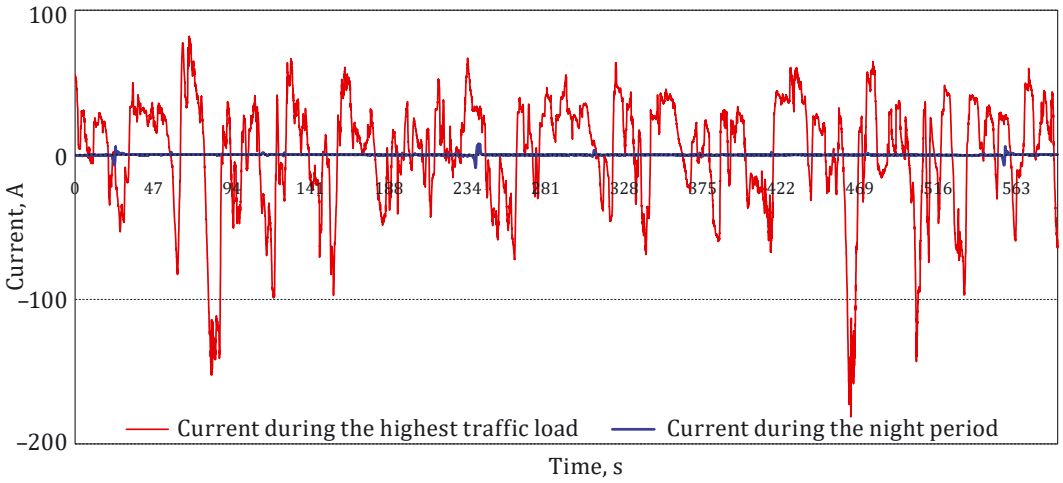

Figure 8. Results of stray current field measurement in the measuring point with very high tram traffic, measurement conducted during the rush hours and at night when tram traffic is not running

4. Rail current measurements

When each electrical substation supplies a particular section of a single tram track, and the traffic load is relatively light, it is possible to detect current losses in some sections of track by simultaneously measuring the current in the rails at several measuring points. These losses correspond to stray currents. This type of measurement was performed in the tram track infrastructure in Ostrava, the Czech Republic. During the measurement, one substation was switched off, so that only the Vresina substation (marked with the letter S in Figure 9)

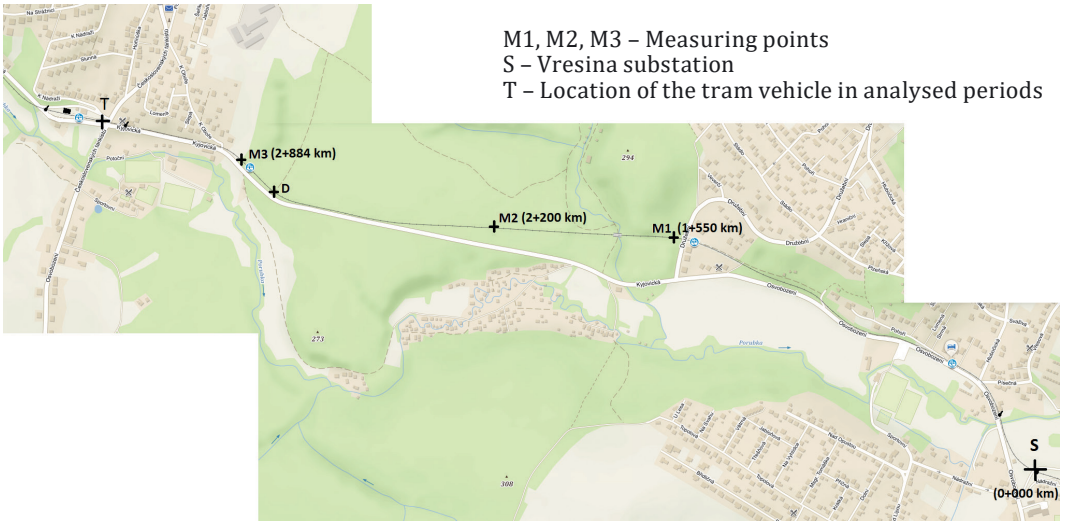

Figure 9. Measuring section at tram track infrastructure in the Ostrava, the Czech Republic

Figure 10. TANGO NF2 Nova tram type (Stadler, 2022)

supplied this section. Unlike many other infrastructures in the world, in Ostrava tram infrastructure, the rails represent the positive pole, and the overhead line is negative. This means that the current to supply the vehicle flows through the rails and the overhead line is used as the return conductor.

The measurement was performed on a 1344 km long measuring section and the current was continuously measured in measuring points at the beginning and at the end of the measuring section (measuring points M1 and M3 in Figure 9). The continuous measurement of the current was performed using laptop computers equipped with input analogue-to-digital converters (16-bit resolution and 10 ks/s) and measuring software created in the LabVIEW system.

During the measurement, the tram type TANGO NF2 Nova (Figure 10) passed the measurement section. This type of tram vehicle uses 600 V

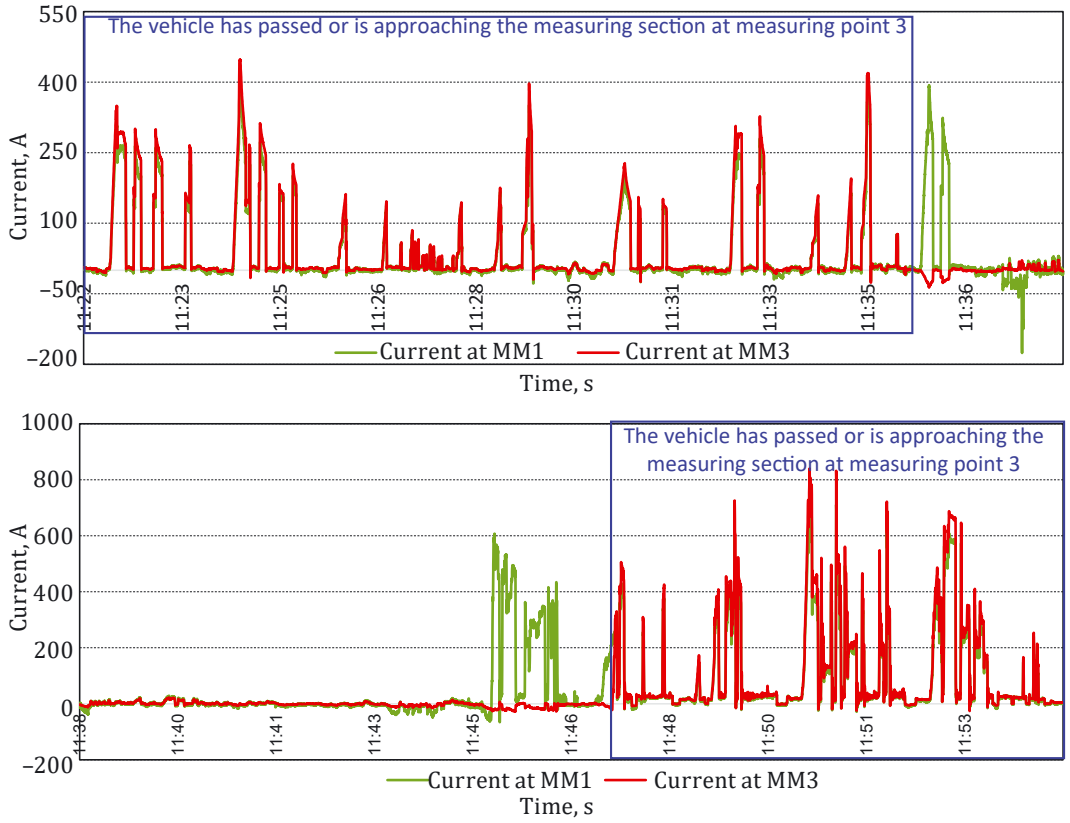

Figure 11. Distribution of current in rails at the measuring points 1 and 3 in time period from 11:22 to 11:53

current for driving. Figure 11 shows time-current diagrams for a 30-minute interval. Analysis of the data has shown that the diagrams have the same shape at the moments when the vehicle leaves or approaches the measurement section and measuring point 3.

As can be seen from Figure 11, the power consumption of the tram vehicle is not continuous. The value of current in the rails and stray current depends on the tramway driving mode – acceleration, deceleration or driving at the same speed, but there are also moments when it is in inertial movement or stops (Chen et al., 2006; Kolář & Hrbáč, 2014). The vehicle consumes the most current when it accelerates, which means that during acceleration the return current in the rails is the highest. Differences between current values in measuring point 1 and 3 represent stray current values in this measuring section.

5. Rail-to-earth potential measurement using the reference electrodes

Mariscotti (2020) analysed the relationship between the track potential distribution and the resulting stray current. He stated that operating conditions of the trains, rail and track bonding and substation distribution had an influence on the potential distribution. The EN 50122-2011 standard describes the measurement of the potential between rail and earth using the reference electrodes. In this type of measurement, one electrode must be placed at a distance of at least 1 m from the rail and the other at a distance of 30 m (Fig. 12). The measurement includes the measuring of the potential between rail and electrode E_1 and the potential between electrodes E_1 and E_2.

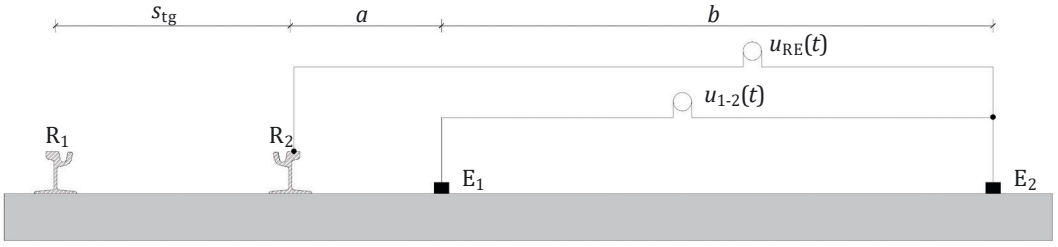

R_1 – rail 1
R_2 – rail 2
E_1 – electrode 1
E_2 – electrode 2
$u_{RE}(t)$ – rail-to-earth potential
$u_{1\text{-}2}(t)$ – potential between electrode E_1 and E_2
a – distance between rail R_2 and electrode E_1
b – distance between rail R_2 and electrode E_2
s_{tg} – gauge width

Figure 12. Rail-to-earth potential measurement according the standard EN 50122:2-2011

Using the measured values, rail-to-earth conductance can be calculated. For the single-track lines local conductance per length is calculated as follows Eq. (1):

$$G'_{\mathrm{RE}} = \frac{m_{\mathrm{sr}} \cdot \pi \cdot 2000}{\rho_{\mathrm{E}} \left[\ln b(b + s_{\mathrm{tg}}) + \ln a(a + s_{\mathrm{tg}}) \right]} \tag{1}$$

For double track electrical conductance can be calculated using the Equation (2):

$$G'_{\mathrm{RE}} = \frac{m_{\mathrm{sr}} \cdot \pi \cdot 1000}{\rho_{\mathrm{E}} \left[\ln \left[(b + 0.5 s_{\mathrm{tg}})(b + 0.5 s_{\mathrm{tg}} + s_{\mathrm{td}}) \right] + \ln \left[(a + 0.5 s_{\mathrm{tg}})(a + 0.5 s_{\mathrm{tg}} + s_{\mathrm{td}}) \right] \right]}, \tag{2}$$

where m_{sr} is stray current transfer ratio; ρ_{E} is the soil resistivity, Ω m; a is the distance between the outer running rail and the remote electrode E_1, m; b is the distance between the outer running rail and the remote electrode E_2, m; s_{tg} is the track gauge, m; s_{td} is distance between parallel tracks, m.

Potential U_{12} needs to be plotted as a function of the rail potential ΔU_{RE}. The slope of the linear regression of this function is the stray current transfer ratio m_{sr}.

Rail-to-earth conductance is of great significance for stray current assessment. Knowing this value, stray current per length can be calculated according to the equation given in the standard, Eq. (3):

$$I'_{\mathrm{S}} = U_{\mathrm{RE}} \cdot G_{\mathrm{RE}}, \tag{3}$$

where U_{RE} is rail potential, and it can be calculated using the equation

$$U_{\mathrm{RE}} = 0.5 \cdot I \cdot R_{\mathrm{C}} \left(1 - e^{-\frac{L}{L_{\mathrm{C}}}} \right),$$

I is the average value of the traction current in the section, R_{C} is the characteristic resistance of the system running rails/structure $R_{\mathrm{C}} = \sqrt{R'_{\mathrm{R}} / G'_{\mathrm{RE}}}$, L_{c} is the characteristic length of the system running rails/structure $L_{\mathrm{C}} = 1 / \sqrt{R'_{\mathrm{R}} G'_{\mathrm{RE}}}$, R'_{R} the longitudinal resistance of the running rails. The rail resistance can be measured and calculated using Ohms law as described by Kolář & Hrbáč (2014).

The rail-to-earth potential measurement with reference electrodes was performed in the city of Ostrava on the tram track section showed in Figure 9. The measurement was performed at all three measuring points (M1, M2 and M3). $Cu/CuSO_4$ reference electrodes were used for the measurement. One electrode was placed 7 m and the other 40 m from the track. The measurement was performed continuously for 2.5 h.

Soil resistivity was measured using the Wenner's method. This method is based on putting four electrodes into the ground at equal distances. A current of a certain strength is conducted into the soil

via two outer electrodes and the voltage is measured at the two inner electrodes ("Watts Current" technical bulletin, 2021; Vidov, 2009). Specific soil resistance is a basic parameter at determination of corrosive aggressiveness. The calculation of the resulting specific soil resistance can be performed using the following equation (Siranec et al., 2019), Eq. (4):

$$\rho = 2\pi \cdot l \cdot R, \tag{4}$$

where l is the pitch of electrodes, m and R is the measured resistance, Ω.

After this measurement, the average values of the rail-to-earth potential U_{RE} and the potential between electrodes U_{12} were calculated. Using the equation defined in the standard, the rail-to-earth conductance was calculated at all three measuring points.

Bongiorno & Mariscotti (2018) gave some practical tips for rail potential field measurements. If it is hard to reach the soil due to asphalt area, concrete electrodes of $CuSO_4$ type may be considered. When the tracks are closed, it is difficult to ensure the connection to the rail, so magnets may be used for this purpose, holding a small flat piece of copper to the side of the rail opposite to where the edge of the wheel is.

Stray current monitoring systems are based on continuous rail-to-earth potential measurements. The rail potential is normally measured in electrical substations and when the measured values change, the rail-to-earth resistance in the section between two substations also changes.

6. Measurement at stray current collection system

If the track is built with a stray current collection system, it can be used to measure the current flow in the collection system. Stray current collection system is providing the low resistance path for the stray current so the current that leaves the rails enters the collection system, rather than nearby infrastructure (Stray DC Current, 2021). Using the collection system corrosion of nearby infrastructure is stopped. The upper layer of reinforcing bars in the concrete track bed may be used as a collection system. Collection system is needed when rail isolation and power-system design themselves cannot keep stray current levels below maximum allowed values (Cotton et al., 2005). According to Charalambous et al. (2016), current can be measured using a shunt resistor installed as part of the transverse bond connection, using the sensor or other suitable means.

Since the collection system is "tightly coupled" to the tracks, it can provide a reasonable estimate of stray current leakage. If the transit system is not operated on a 24-hour basis to obtain more accurate data,

a test tram can be used. In this case, measurements should be made while a single train is traveling through the area of interest, pausing at passenger stations, and then accelerating at full power to normal speed between stations. It is good practice to perform the tests with the test train running once in each direction through the area of interest.

7. Non-destructive sensors

Stray current on metal objects near urban track infrastructure can be measured with non-destructive sensors. Peelen et al. (2011) described the non-destructive measurement of stray current on sheet piles near railway infrastructure. Stray current from the railway enters and leaves the sheet pile wall, resulting in changes in corrosion current density and electrical potential between the steel and the soil. The authors used two types of sensors – a coupon sensor, which provides information about the local stray current density, and a reference electrode, which is used to measure the electrical potential differences between the electrode and the soil near the coupon sensor. A coupon sensor is a small steel plate made of the same material as the sheet pile and attached to the sheet pile in such a way that it is electrically isolated. The plate is electrically connected to the sheet pile wall via a zero-ohm ammeter so that it is possible to measure the current entering or leaving the steel coupon (Peelen et al., 2011). Mariscotti (2009) described a sensor for non-invasive measurement of rail current. This sensor is designed to detect the magnetic field generated by the rail current. Xu et al. (2014) described a stray current sensor for buried pipelines. The sensor is connected to the pipeline through a connector. Through this connection, the stray current from the pipeline can enter the sensor and be detected there.

Continuous stray current monitoring systems that are in use in urban tracks worldwide also use non-destructive sensors. For example, continuous potential monitoring with the permanent reference electrode buried during track construction uses a stray current sensor to measure the potential difference between the object and the electrode (Peng et al., 2020).

Conclusion

Given the high density of rail traffic in urban areas, corrosion from stray currents is an increasing problem for rail infrastructure and adjacent structures. Many operators around the world have recognized this problem and have taken measures to reduce stray currents, which

can be divided into two groups: i) ensuring a low longitudinal electrical resistance of the rail, ii) increasing the electrical resistance between the rail and the ground. The low value of longitudinal rail resistance can be achieved by using rails with larger cross-section and ensuring continuous connection of rails, i.e., welding. When it comes to electrical resistance between the rails and the ground, the most important element is the insulation of the rail. In discretely supported and fastened tracks, where it is extremely difficult to completely insulate the rails, the high value of this electrical resistance can be achieved by efficient track drainage to avoid water accumulation in the track and by choosing a fastening system with high electrical resistance. In discretely supported and fastened track, the fastening points are "discharge points" of current, i.e., locations where current can flow from the rail through the fasteners into the lower layers of the track structure. Thus, by using a better insulated fastening system, this current flow can be reduced.

The presence of stray currents on the track and surrounding metal structures can be detected by various field measurement methods. Stray currents due to tram traffic are dynamic and depend on many factors. The most important ones are the density of tram traffic, the mode of operation, and the electrical resistance between the rail and the ground, which depends on the insulation of the rails and fasteners, track maintenance, and soil moisture – moist soil has lower electrical resistance. For this reason, the results of field measurements taken at the same location and at different times can be different. To get a clear picture of the hazard of stray currents on an observed section of track, measurements should be made at several time intervals or continuous monitoring of stray currents on the track should be established. Such monitoring is nowadays mostly based on continuous monitoring of the rail potential. Today, there are no applicable standards prescribing ways to control and monitor corrosion and stray currents on tracks, and all methods used today depend on the operator. The effect of corrosion on track is still an area that does not receive enough attention, and the harmful consequences that corrosion can cause are not taken seriously enough.

Acknowledgements

The research was carried out in cooperation with the following institutions: University of Zagreb, Faculty of Civil Engineering, University of Ostrava, Faculty of Electrical Engineering and Computer Science, University of Genoa, Department of Electrical, Electronic and Telecommunications Engineering, and Naval Architecture.

REFERENCES

Alamuti, M. M., Nouri, H. & Jamali, S. (2011). Effects of earthing systems on stray current for corrosion and safety behaviour in practical metro systems. *IET Electrical Systems in Transportation*, *1*(2), 69–79. https://doi.org/10.1049/iet-est.2010.0029

Alar, V. (2015). Kemijska postojanost metala, University of Zagreb. https://bib.irb.hr/datoteka/843434.KEMIJSKA_POSTOJANOST.pdf

Bongiorno, J. & Mariscotti, A. (2015). Accuracy of railway track conductance and joint efficiency measurement methods. *Acta Imeko*, *4*(4), 82–87. https://doi.org/10.21014/acta_imeko.v4i4.270

Bongiorno, J. & Mariscotti, A. (2018). Track insulation verification and measurement. *MATEC Web of Conferences*, *180*, Article 01008. https://doi.org/10.1051/matecconf/201818001008

Charalambous, C. A. (2005). Stray current control and corrosion for DC mass transit systems [PhD thesis, University of Manchester].

Charalambous, C. A. (2017). Comprehensive modelling to allow informed calculation of DC traction systems' stray current levels. *IEEE Transactions on Vehicular Technology*, *66*(11), 9667–9677. https://doi.org/10.1109/TVT.2017.2748988

Charalambous, C. A., Aylott, P. & Buxton, D. (2016). Stray current calculation and monitoring in DC mass-transit systems: Interpreting calculations for real-life conditions and determining appropriate safety margins. *IEEE Vehicular Technology Magazine*, *11*(2), 24–31. https://doi.org/10.1109/MVT.2015.2477419

Chen, S. L., Hsu, S. C., Tseng, C. T., Yan, K. H., Chou, C. Y., & Too, T. M. (2006). Analysis of rail potential and stray current for Taipei Metro. *IEEE Transactions on Vehicular Technology*, *55*(1), 67–75. https://doi.org/10.1109/TVT.2005.861164

Chen, Z., Koleva, D., & van Breugel, K. (2017): A review on stray current-induced steel corrosion in infrastructure. *Corrosion Reviews*, *35*(6), 397–423. https://doi.org/10.1515/corrrev-2017-0009

Cotton, I., Charalambous, C., Aylott, P., & Ernst, P. (2005). Stray current control in DC mass transit systems. *IEEE Transactions on Vehicular Technology*, *54*(2), 722–730. https://doi.org/10.1109/TVT.2004.842462

Darowicki, K., & Zakowski, K. (2004). A new time-frequency detection method of stray current field interference on metal structures. *Corrosion Science*, *46*(5), 1061–1070. https://doi.org/10.1016/j.corsci.2003.09.007

Dolara, A., & Leva, S. (2009). Calculation of rail internal impedance by using finite elements methods and complex magnetic permeability. *International Journal of Vehicular Technology*, *2009*, Article 505246. https://doi.org/10.1155/2009/505246

Du, G., Zhang, D., Li, G., Wang, C., & Liu, J. (2016). Evaluation of rail potential based on power distribution in DC traction power systems. *Energies*, *9*(9), 729–749. https://doi.org/10.3390/en9090729

Haladin, I., Lakušić, S. & Bogut, M. (2019). Overview and analysis of methods for assessing ride comfort on tram tracks. *GRAĐEVINAR*, *71*(10), 901–921. https://doi.org/10.14256/JCE.2731.2019

Haladin, I., Bogut, M. & Lakušić, S. (2021). Analysis of tram traffic-induced vibration influence on earthquake damaged buildings. *Buildings*, *11*(12), Article 590. https://www.mdpi.com/2075-5309/11/12/590

Hill, R. J., & Cai, Y. (1993). Simulation of rail voltage and earth current in a PC-based traction power simulator. *Transactions on Engineering Sciences*, *3*, 319–326.

Isozaki, H., Oosawa, J., Kawano, Y., Hirasawa, R., Kubota, S., & Konishi, S. (2016). Measures against electrolytic rail corrosion in Tokyo metro subway tunnels. *Procedia Engineering*, *165*, 583–592. https://doi.org/10.1016/j.proeng.2016.11.754

Ivanković, A, Martinez, S., & Kekez, K., (2009). Stray current detection on hazardous liquid buried pipelines as a part of pipeline integrity management. *3rd International Symposium on Environmental Management*, Book of Abstracts, Croatia.

Ivanković, A., Martinez, S., & Kekez, K. (2011). Detekcija štetnih učinaka statičkih i dinamičkih lutajućih struja SCM uređajem. *Proceedings of the 13 YUCORR International conference Exchanging experiences in the fields of corrosion, materials and environmental protection*: Serbia.

Kolář, V., & Hrbáč, R. (2014). Measurement of ground currents leaking from DC electric traction. *Proceedings of the 15th International Scientific Conference on Electric Power Engineering*, Brno-Bystrc, Czech Republic, 613–617. https://doi.org/10.1109/EPE.2014.6839423

Krajcar, S. et al. (2009). Elektroenergetska studija tramvajske mreže grada Zagreba Elektroenergetska studija tramvajske mreže grada Zagreba, University of Zagreb, Faculty of Electrical Engineering and Computing.

Mariscotti, A. (2009). Rail current measurement with noninvasive large dynamic probe. *IEEE Transactions on Instrumentation and Measurement*, *58*(5), 1610–1616. https://doi.org/10.1109/TIM.2009.2014508

Mariscotti, A., Reggiani, U., Ogunsola, A., & Sandrolini, L. (2012). Mitigation of electromagnetic interference generated by stray current from a dc rail traction system. *IEEE International Symposium on Electromagnetic Compatibility,* Rome, Italy, 1–6. https://doi.org/10.1109/EMCEurope.2012.6396805

Mariscotti, A. (2020). Stray current protection and monitoring systems: Characteristic quantities, assessment of performance and verification. *Sensors*, *20*(22), Article 6610. https://doi.org/10.3390/s20226610

Mariscotti, A. (2021a). Electrical safety and stray current protection with platform screen doors in DC rapid transit. *IEEE Transactions on Transportation Electrification*, *7*(3), 1724–1732. https://doi.org/10.1109/TTE.2021.3051102

Mariscotti, A. (2021b). Impact of rail impedance intrinsic variability on railway system operation, EMC and safety. *International Journal of Electrical and Computer Engineering*, *11*(1), 17–26. https://doi.org/10.11591/ijece.v11i1.pp17-26

Milesevic, B., Filipovic-Grcic, B., Uglesic, I., & Jurisic, B. (2018). Estimation of current distribution in the electric railway system in the EMTP-RV. *Electric Power Systems Research*, *162*, 83–88. https://doi.org/10.1016/j.epsr.2018.05.004

Ooagu, R., Taguchi, K., Yashiro, Y., Amari, S., Naito H., & Hayashiya, H. (2019). Measurements and calculations of rail potential in D.C. traction power supply system. *11th Asia-Pacific International Conference on Lightning*, Hong Kong, China, 1–6. https://doi.org/10.1109/APL.2019.8816070

Ovchinnikov, D., Bondarenko, A., Kou, L. & Sysyn, M. (2021). Extending service life of rails in the case of a rail head defect. *GRAĐEVINAR*, *73*(2), 119–125. https://doi.org/10.14256/JCE.2860.2019

Panda, B., Balasubramaniam, R., & Dwivedi, G. (2008). On the corrosion behaviour of novel high carbon rail steels in simulated cyclic wet-dry salt fog conditions. *Corrosion Science*, *50*(6), 1684–1692. https://doi.org/10.1016/j.corsci.2008.02.021

Pathak, M., Alahakoon, S., Spiryagin, M., & Cole, C. (2019). Rail foot flaw detection based on a laser induced ultrasonic guided wave method. *Measurement*, *148*, Article 106922. https://doi.org/10.1016/j.measurement.2019.106922

Peelen, W. H. A., Neeft, E., Leegwater, G., Van Kanten-Roos, W., & Courage, W.M.G. (2011). Monitoring DC stray current interference of steel sheet pile structures in railway environment. *Heron*, *56*(3), 107–122. http://heronjournal.nl/56-3/2.pdf

Peng, P., Zeng, X., Leng, Y., Yu, K., & Ni, Y. (2020). A new on-line monitoring method for stray current of DC metro system. *IEEJ Transactions on Electrical and Electronic Engineering*, *15*(10), 1482–1492. https://doi.org/10.1002/tee.23219

"Watts Current" technical bulletin. (2021, September 14). *Performing a Wenner soil resistivity test with the AEMC Model 6472*. https://www.aemc.com/userfiles/files/resources/applications/ground/APP_Wenner.pdf

Radiodetection. (2011). *Stray current mapper user manual*. https://www.radiodetection.com/sites/default/files/UG058EN_02%20SCM%20User%20Guide.pdf

Ritter, G. W., Stuart, C. & Tang, Y. (2018). Rail Base Corrosion and Cracking Prevention: Phase 2, https://rosap.ntl.bts.gov/view/dot/35437

Robles Hernández, F. C., Plascencia, G., & Koch, K. (2009). Rail base corrosion problem for North American transit systems. *Engineering Failure Analysis*, *16*(1), 281–294. https://doi.org/10.1016/j.engfailanal.2008.05.011

Safa, M., Sabet, A., Ghahremani, K., Haas, C., & Walbridge, S. (2015). Rail corrosion forensics using 3D imaging and finite element analysis. *International Journal of Rail Transportation*, *3*(3), 164–178. https://doi.org/10.1080/23248378.2015.1054622

Samal, S., Bhattaacharyya, A., & Mitra, S. K. (2011). Study on corrosion behaviour of pearlitic rail steel. *Journal of Minerals and Materials Characterization and Engineering*, *10*(7), 573–581. https://doi.org/10.4236/jmmce.2011.107044

Siranec, M., Regula, M., Otcenasova, A., & Altus, J. (2019). Measurement and analysis of stray currents. *Proceedings of the 2019 20th International Scientific Conference on Electric Power Engineering, EPE 2019*, Kouty nad Desnou, Czech Republic, 4–9. https://doi.org/10.1109/EPE.2019.8778072

Stadler. (2022). *Stadler Tango NF2*. https://sk.wikipedia.org/wiki/Stadler_Tango_NF2

Steimel, A. (2012). Power-electronic grid supply of AC railway systems. *Proceedings of the International Conference on Optimisation of Electrical and Electronic Equipment, OPTIM*, Brasov, Romania, 16–25. https://doi.org/10.1109/OPTIM.2012.6231844

Hartenergy. (2021, May 28). *Stray current mapper*. https://www.hartenergy.com/news/stray-current-mapper-51812

Stray DC Current. (2021, June 4). *Stray DC Current*. http://www.railsystem.net/stray-dc-current

TCRP. (2016). Guidelines for rail base inspection and rail condemnation limits for corrosion-induced material loss. https://www.nap.edu/catalog/21941/guidelines-for-rail-base-inspection-and-rail-condemnation-limits-for-corrosion-induced-material-loss

Vidov, V. (2009). Utjecaj parametara tla i lutajućih struja na koroziju podzemnih građevina [master thesis, University of Zagreb].

Vranešić, K., Lakušić, S., & Serdar, M. (2020), Corrosion and stray currents at urban track infrastructure. *GRAĐEVINAR*, *72*(7), 593–606. https://doi.org/10.14256/JCE.2909.2020

Wang, M., Yang, X., Zheng, T. Q., & Ni, M. (2020). DC autotransformer-based traction power supply for urban transit rail potential and stray current mitigation. *IEEE Transactions on Transportation Electrification*, *6*(2), 762–773. https://doi.org/10.1109/TTE.2020.2979020

WebCorr. (2021, May 28). *Different types of corrosion*. https://www.corrosionclinic.com

Xu, S., Li, W., Wang, Y., & Xing, F. (2014). Stray current sensor with cylindrical twisted fiber. *Applied Optics*, *53*(24), 5486–5492. https://doi.org/10.1364/AO.53.005486

Xu, S. Y., Li, W., & Wang, Y. Q. (2013). Effects of vehicle running mode on rail potential and stray current in DC mass transit systems. *IEEE Transactions on Vehicular Technology*, *62*(8), 3569–3580. https://doi.org/10.1109/TVT.2013.2265093

Xu, W., Zhang, B., Deng, Y., Wang, Z., Jiang, Q., Yang, L., & Zhang, J. (2021). Corrosion of rail tracks and their protection. *Corrosion Reviews*, *39*(1), 1–13. https://doi.org/10.1515/corrrev-2020-0069

Zaboli, A., Vahidi, B., Yousefi, S., & Hosseini-Biyouki, M. M. (2017). Evaluation and control of stray current in DC-electrified railway systems. *IEEE Transactions on Vehicular Technology*, *66*(2), 974–980. https://doi.org/10.1109/TVT.2016.2555485

Zhang, D. (2012). Research on technical measure for rail potential reduction. *Applied Mechanics and Materials*, *155–156*, 181–185. https://doi.org/10.4028/www.scientific.net/AMM.155-156.181